PROCEEDINGS, 47th Workshop on Geothermal Reservoir Engineering
Stanford University, Stanford, California, February 7-9, 2022
SGP-TR-223

Technical and Economic Evaluation of a Geothermal field in a Sedimentary Basin on the Texas Gulf Coast

Cesar Vivas[1], Danny Rehg[2], Laura Ortiz[1], Denise Knight[2], Stephanie Perry[3], Adam Bradley[2], Saeed Salehi[1] and Sean Marshall[2].

The University of Oklahoma, Norman, OK, USA[1], Criterion Energy Partners, Houston, TX, USA[2], Geomark, Houston, TX, USA[3]

cesar.vivas@ou.edu

Keywords: Reservoir Modeling, Geothermal Energy, Enthalpy Production, Sedimentary Basin

ABSTRACT

Geothermal energy is an appealing source of baseload renewable energy capable of supplying constant energy regardless of seasonal and other environmental factors. Benefiting from subsurface natural heat anomalies, geothermal energy projects have been developed primarily on igneous and metamorphic environments where temperature gradients are elevated near the surface. Hard rock combined with high temperatures and a corrosive environment makes geothermal drilling difficult and expensive. However, the access to hot reservoirs is not limited to igneous and metamorphic environments. Fields with downhole temperatures of 150°C and above are present in reservoirs 3 to 4 km depth in sedimentary basins in the US. Sedimentary environments have the advantage of large quantities of existing subsurface datasets and lower cost to drill. Additionally, the porosity and permeability in sedimentary basins are more favorable than traditional geothermal reservoirs, allowing for improved flow potential and heat extraction.

In this paper, a technical, economic evaluation is performed to ascertain the potential geothermal development in a sedimentary field in the Gulf Coast area in Texas. Various reservoir simulations with different wells configurations were analyzed. Furthermore, the use of existing oil and gas wells, combined with new vertical and horizontal wells, is evaluated. A sensitivity analysis indicates that permeability and fracture density affect the heating extraction rate. Also, the variation in the wells' position and configuration affect the energy production. Finally, we conclude that the project of heat extraction for power generation in the area evaluated is technically feasible.

1. INTRODUCTION

Geothermal energy is one of the most reliable renewable energy sources that benefits from the heat stored under the earth's surface. High-temperature geothermal resources placed in volcanic rock reservoirs are mainly used for power generation. Until now, the use of this energy in the world has developed in areas with high-temperature hydrothermal resources. But current technological advances in equipment and improvements in prospecting and drilling allow geothermal today to have the technology for producing electricity from geothermal resources with notably lower temperatures than those required years ago.

Geothermal resources are not limited to volcanic environments. Sedimentary basins store massive amounts of thermal energy by heat conducted from the earth's lower crust during the sedimentary rock lithification process (Bethke et al., 1988). Sedimentary basins present a potential new pathway toward geothermal energy production expansion. The use of known porous and permeable reservoir rocks in sedimentary basins, where the reservoirs have sufficient temperature, thickness, porosity, and permeability, can expand the geothermal energy generation to new areas in the United States (Anderson, 2013). The development of geothermal projects in deep sedimentary basins offers multiple advantages compared with traditional geothermal exploration targets. Some deep reservoirs, particularly in oil and gas sedimentary basins, contain significant exploration data (core, seismic, logs, etc.) that helps their proper characterization. Additionally, the wellbore construction can benefit from the oil and gas vast experience in developing the know sedimentary reservoirs. Drilling known sedimentary basins are less risky, potentially faster, and less expensive than geothermal drilling in igneous and metamorphic rocks. This is particularly important, considering that around 50% of the capital cost of a geothermal plant is attributed to the drilling costs of the geothermal wells (Vivas et al., 2020).

Another advantage of exploring sedimentary basins is the accessibility to inactive oil and gas wells, which can reduce the impact of the well construction costs in geothermal developments. The concept of using existing oil and gas wells have been analyzed by several authors (Kujawa et al., 2004, Bu et al., 2012, Chen et al., 2013, Caulk and Tomac, 2017, Gharibi et al. 2018). Davis and Michaelides (2009) evaluated using existing oil and gas wells in south Texas, concluding that wells 3 km deep can potentially produce 2-3 MW of power. Wight and Bennett (2015) evaluated the logs of over 2500 existing wells in Texas, finding that wells with reservoir temperatures of 130°C are capable of producing geothermal power.

This study analyzes the usage of existing oil and gas wells in a sedimentary basin in Texas Gulf Coast. The novelty of this approach is the combined use of existing oil and gas wells as injector wells, and a new horizontal well for production. To assess the potential of the project, logs from existing wells in the area were used to build the reservoir model. Petrophysical properties combined with geothermal gradient data were used as input to determine potential new well locations. This enables to evaluate the impact of well positioning in the energy output of the project.

2. TEXAS GULF COAST BASIN GEOLOGY

The area of focus is the Texas Gulf Coast basin embayment (Fig. 1 a). This region consists of contemporaneous deltaic deposition, faulting and movement of deep salt domes which resulted in the accumulation of hundreds of feet of sandstone in the Frio formation. This buildup is composed of several generally coarsening upward sequences that consists of pro-delta shale at the base, delta-front shale and sand in the middle, and delta-plain sandstone and shale at the top (Fig. 1 b).

a)

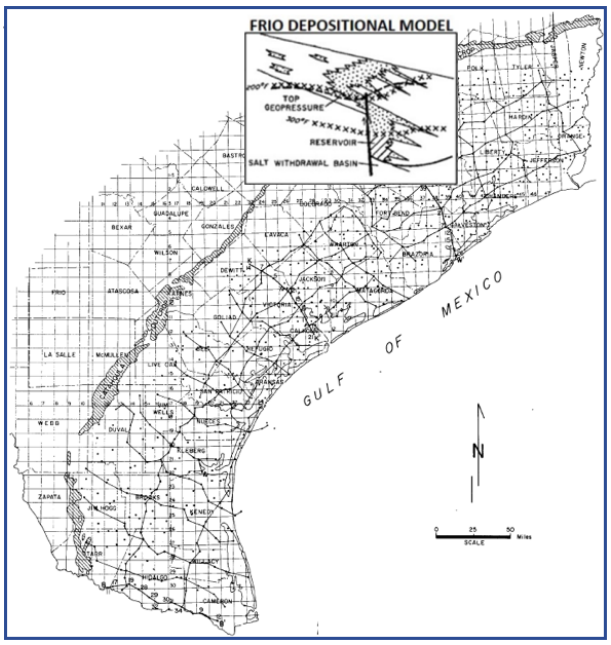

b)

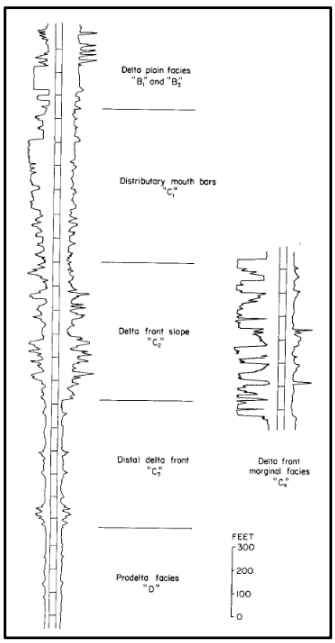

Figure 1: (a) Texas Gulf Coast depositional model (modified from Bebout et al., 1978), and (b) Depositional environments of a high-constructive lobate delta system interpreted from electrical log patterns (after Fisher, 1969).

The geothermal reservoir of interest is the Frio which is Tertiary in age and is stratigraphically above the Vicksburg and below the Anahuac formations (Fig. 2a). Faults in the area are controlled by massive deltaic deposition and salt movement. Due to salt movement, rapid subsidence occurred allowing for thick sections of sand and shale to deposit initiating the formation of growth faults (Fig. 2b).

a)

SYSTEM	SERIES	GROUP/FORMATION
Quaternary	Recent Pleistocene	Undifferentiated Houston
Tertiary	Pliocene	Goliad
	Miocene	Fleming
	?——?	Anahuac
	Oligocene	Frio
		Vicksburg
	Eocene	Jackson
		Claiborne
		Wilcox
		Midway

b)

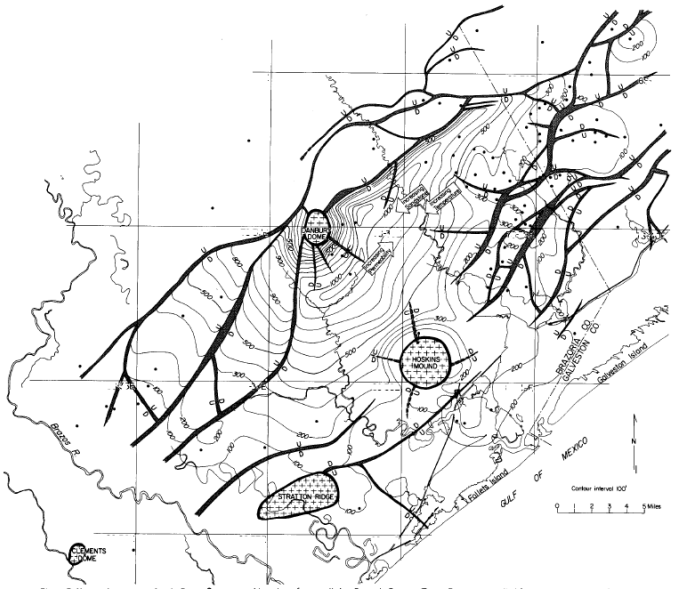

Figure 2: (a) Stratigraphic section, Texas Gulf Coast, and (b) Structure on top of the Frio T5 Marker (Bebout et al., 1978).

3. RESERVOR MODEL CHARACTERIZATION

3.1 Petrophysical Properties

In this study ~25 wells were utilized to investigate and constrain the regional and localized property distributions. First, wells that met a minimum requirement of an open hole wireline triple combination log suite was required. The triple combination criteria includes a gamma ray (GR-GAPI), if present a caliper (CALI-inches), if present spontaneous potential (SP-mV), resistivity (RDEEP-ohms), bulk density (RHOB- g/cc), neutron porosity (NPHI- v/v) and if present a photoelectric factor (PE- b/e) (Fig. 3). If bulk density (g/cc) was not available/present than a monopole compressional sonic or delta-T log was required (DT- us/ft).

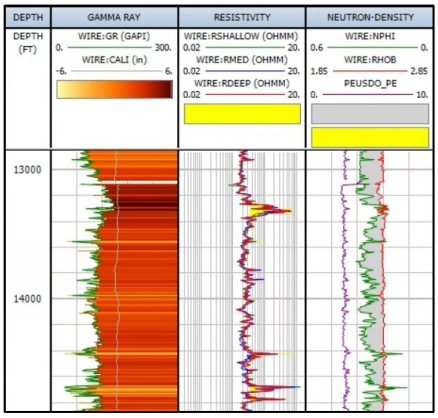

Figure 3: Example of a required triple combination log for petrophysical evaluation.

Before petrophysical evaluation, logs were checked for quality, identifying where the nuclear measurements were invalid due to borehole or environmental effects. If the logs were impacted by poor borehole quality and washout on the bulk density (g/cc) log was identified, then the logs were not used in the evaluation.

The objectives of the petrophysical evaluation were to evaluate the presence and quality of the reservoir for both injection capacity and geothermal production capacity. To do so the following properties were evaluated:

- Reservoir presence - Sandstone versus clay versus carbonate volume
- Reservoir Container Capacity – Total Porosity
- Fluid Type Presence – Total Water Saturation
- Reservoir Flow Capability – Permeability

For reservoir presence a combination of the gamma ray (gapi) and bulk density (g/cc) -to neutron porosity (v/v) separation were utilized. Where on the GR the clean sandstone baseline was set at ~35-40 gapi and the 'clay' baseline ranged from 180-220 gapi. No gamma ray normalization was applied prior to the volume of clay (VCL) interpretation (Fig. 4). The volume of clay was used for quick look screening to identify the presence or lack thereof sandstone thickness (minimum criteria of ~10 feet). The gamma ray was also used by the petrophysicist and geologist collaboratively to correlate parasequence stratigraphy. In addition, the separation between the bulk density (g/cc) and neutron porosity (v/v) was used to assess the volume of shale. The more significant or increase in separation the more the increase in shale presence.

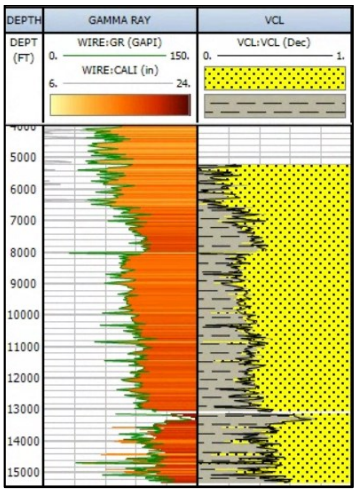

Figure 4: Example of the volume of clay interpretation over the wellbore open-hole wireline logs present.

Moving beyond the sandstone versus clay evaluation, a full multimineral deterministic model was developed and applied. Where a density-neutron cross-plot and the photoelectric factor logs were utilized for constraining the mineralogical end members grain density inputs. In cases where no raw photoelectric factor (PE-b/e) logs were available to use, a pseudo correlation between bulk density and photoelectric factor (Pseudo_PE) in a measurement constrained well was developed. The equation used is as follows:

$$Y = 0.511105643 * e^{(0.72130789 * \mathrm{WIRE:RHOB})} \quad (1)$$

No digitized whole core data or sidewall core data was publicly available for the stratigraphic column in this spatial location. Analog data sets and geological knowledge was used to justify and cross-check the petrophysical inputs and resulting deliverables. Quartz = Sandstone and was set to 2.65 g/cc over the majority of the stratigraphic column except for the Wilcox sandstone. The Wilcox grain density utilized for quartz was 2.68 g/cc. Where Clay=Illite or Mixed Illite/Mica or Mixed Illite/Smectite and the associated dry grain density set to 2.70 g/cc. Limestone = Carbonate was set to 2.71 and Dolomite = Carbonate set to 2.83 g/cc (Fig. 5).

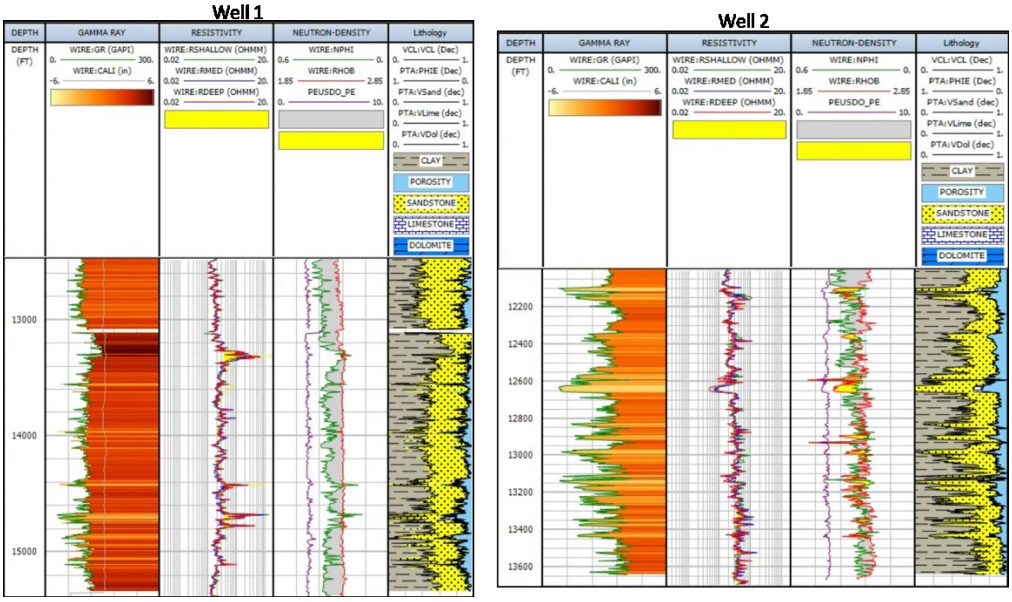

Figure 5: Two well example of the developed and applied multi-mineral model for the project. Tracks left to right include: Depth (Feet-FT), Gamma Ray (GR-Gapi) and caliper (CALI-in), resistivity (RDEEP-RMED-RSHALLOW-ohms), Bulk Density (RHOB-g/cc) and Neutron Porosity (NPHI- v/v) and Photoelectric factor (PE-b/e), and last the multi-mineral model results (Volume of Clay=VCL, Volume of Sandstone=Vsand, Volume of Carbonate = VLIME, Volume of Dolomite=Vdol, Bulk Volume Water=BVW and Effective Porosity=PHIE). Nuclear track (4th from left) including RHOB and NPHI, is set to sandstone matrix scale.

For net sandstone characterization the following criteria can be used to identify and isolate the higher quality sandstones in the stratigraphic column:

- Apply a GR cutoff of <=65 gapi OR apply a Vsand cutoff of >=55% (0.55 v/v) And vertical thickness of >= 10 ft

Once the multi-mineral model is established and extrapolated a best fit total porosity can be calculated from the resulting variable grain density log. At every 0.5 increment the multi-mineral model applied results in a variable grain density log that can be input into the total porosity equation. The multi-mineral model can also be cross-checked with a more simplified density porosity, neutron porosity or porosity derivation. However, the differentiation or strength of the multi-mineral model is that the matrix end member is not a fixed assumed number along the vertical length of the calculation. The matric (RHOG) is allowed to vary as described above. The following equation was used to evaluate the total porosity, where the fluid density is assumed to be 1 g/cc:

$$PHIT = \frac{\rho_{matrix}\,(input\ log) - \rho_{bulk\ volume}\,(input\ log)}{\rho_{matrix}\,(input\ log) - \rho_{fluid}\,(input\ log)} \quad (2)$$

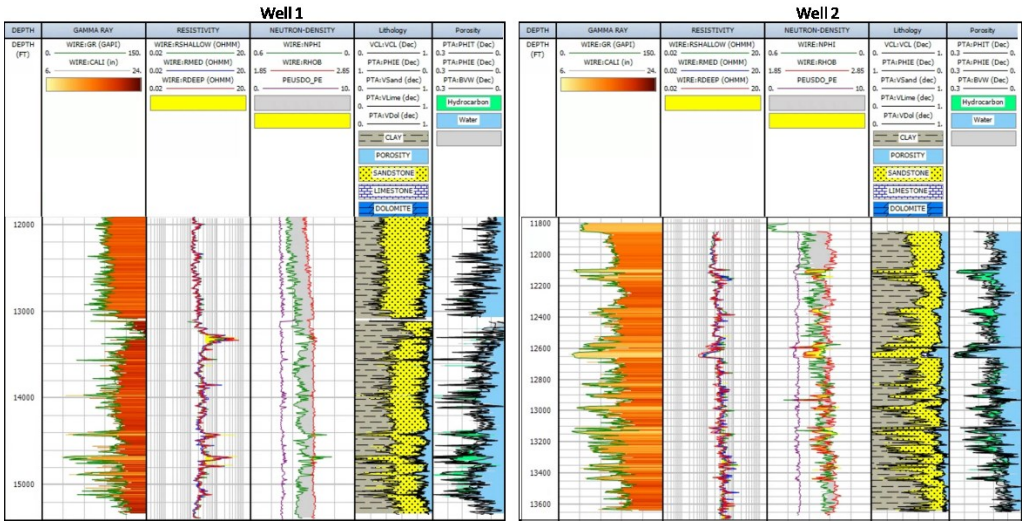

Figure 6: Two well example of the petrophysical evaluation progression. Last track on the right now displays the evaluated total porosity (PHIT), effective porosity (PHIE) and bulk volume water (BVW).

Once total porosity s evaluated, we can now determine the net reservoir over the stratigraphic zones of interest. By applying a cutoff of >= 12% (0.12 v/v) we can highlight the stratigraphy with enough potential storage volume to be of interest for injection and production. By applying a higher, harsher cutoff of >=15% (0.15 v/v), the highest quality sandstones can be identified. The total porosity cutoff stand alone is not adequate to isolate the highest quality reservoir. We must also include a permeability threshold correlated with the porosity log.

The correlation between porosity and permeability was determined from non-digitized literature where a range of the flow capacity in the target of interest sandstones was communicated (Morton, 1979). In addition, an analog formation located in the Permian shallow stratigraphy was deemed equitable in depositional setting, and property distribution. In the analog formation, known measure porosity-permeability correlations can be utilized (Fig. 7). The below equation was used to calibrate, constrain and extrapolate across the wells in the project:

$$\text{Permeability} = 0.0016 * e^{(42.58217 * \text{PTA:PHIT})} \quad (3)$$

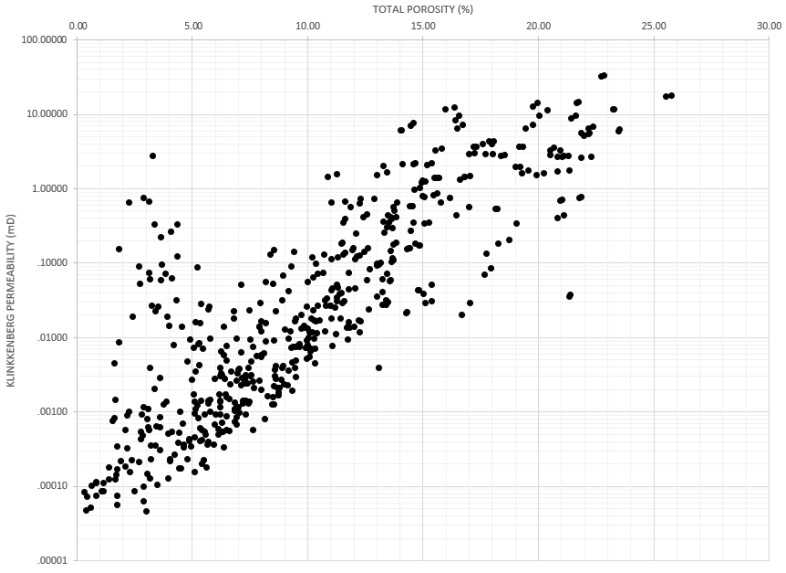

Figure 7: Core plug measured porosity and permeability from analog sandstone in the Permian basin. X-axis is total porosity. Y-axis is Klinkenberg permeability (mD).

Now that we have both total porosity and permeability in mD evaluated across the reservoir sandstones, we can apply additional cutoff flags. These flags aid in identifying the nest quality rock to use from a geological, petrophysical, geophysical, and modelling perspective to achieve the goals of the project. In the below figure we highlight the best quality sandstones by a porosity flag of >=12% and a permeability cutoff of >=5 mD (Fig. 8 and Fig. 9).

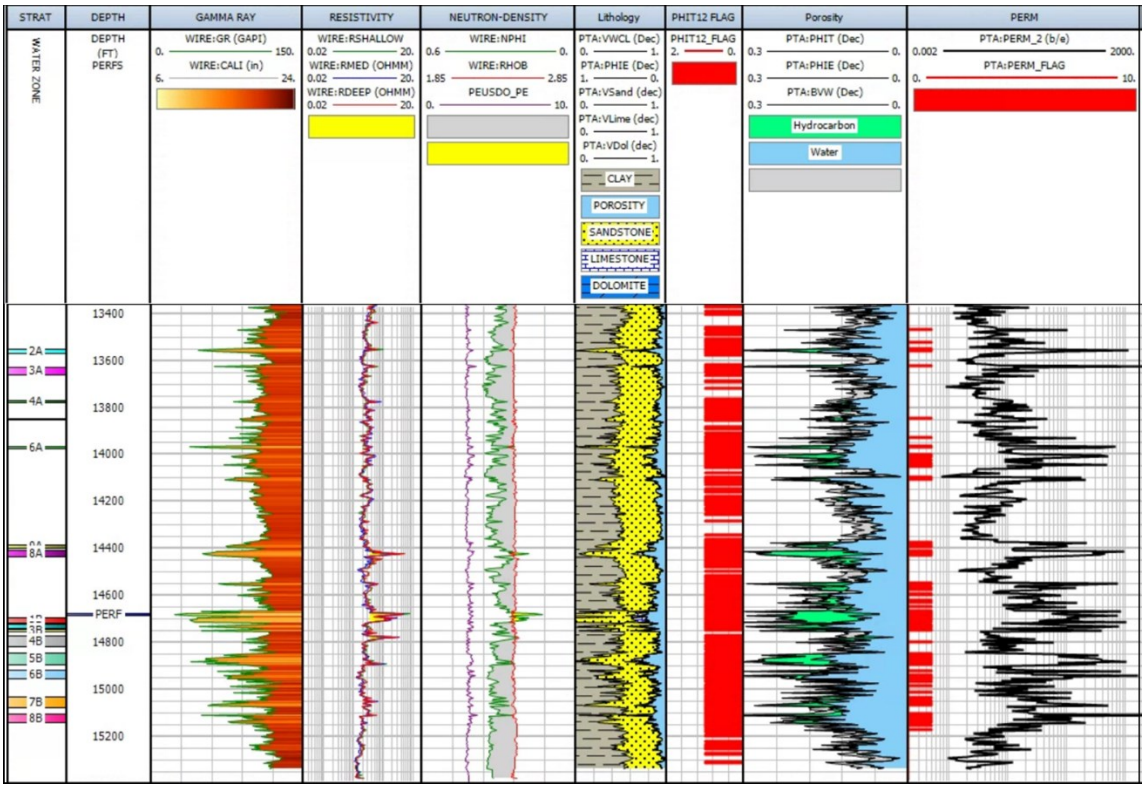

Figure 8: Display of petrophysical evaluation across the reservoirs of interest. Highlighted are the sections of the evaluation where total porosity is >= 12% and permeability is >=5 mD.

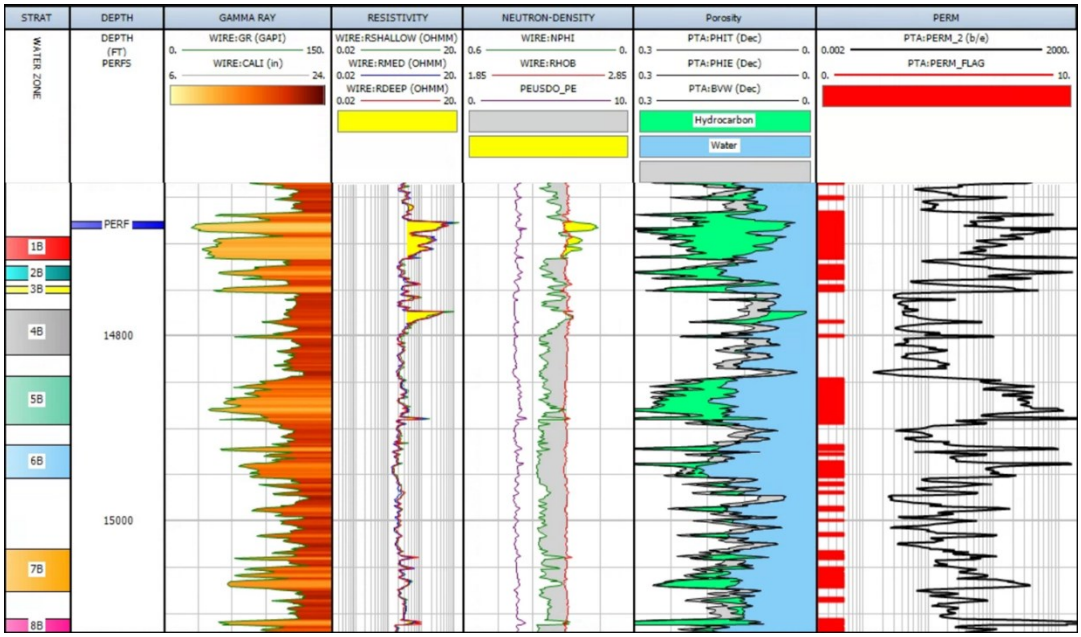

Figure 9: Finer-scale view of potential injection and production zones. This well has previous production through one perforated interval at ~13,800' as noted. The far-right track displays the interpreted permeability with a flag for anything >=5 mD thereby discounting/not including the higher clay-prone interbedded intervals.

The final effort in characterizing the reservoirs is to interpret total water saturation. By doing so we can identify where in the stratigraphic column there is potential for water versus hydrocarbon presence in the known container (total porosity defined). Since we are focused on geothermal applicability we are trying to identify where there is a higher probability of water. Coupled with the geological interpretation of the temperature gradient we can assume that any water *in situ* will meet the criteria for geothermal energy generation. The total water

saturation has the highest range of uncertainty in the petrophysical evaluation and therefore we ran multiple case scenarios of outcomes to constrain the possible outcomes (deterministically).

For this study total water saturation was interpreted via Archie's equation in the standard form expressed as (Archie, 1952):

$$S_{w^n} = \frac{R_W}{PHIT^m * Resistivity\,(True - R_t)} \qquad (4)$$

- Where n = saturation exponent
- R_w = Resistivity of water, either calibrated by water composition measurements, interpreted from a fully water saturated bearing sandstone or a Hingle/Pickett plot is used
- PHIT = Total Porosity
- m = cementation exponent
- R_t = deep resistivity measurement

From Morton, 1979 the salinity range of the formation is ~100-160k ppm. At 60F and translating that salinity to an apparent Rw that provides us with a range of 0.06-0.11 ohms across the wells of interest. The saturation exponent and cementation exponents are not constrained by electrical property core measurements. Rather we assumed standard values for a porous, non-diagenetically altered onshore Gulf of Mexico equivalent sandstone. Therefore n=1.85 and m=1.85. We held these inputs constant and only ranged the Rw to address the uncertainty in the total water saturation results (Figure 10).

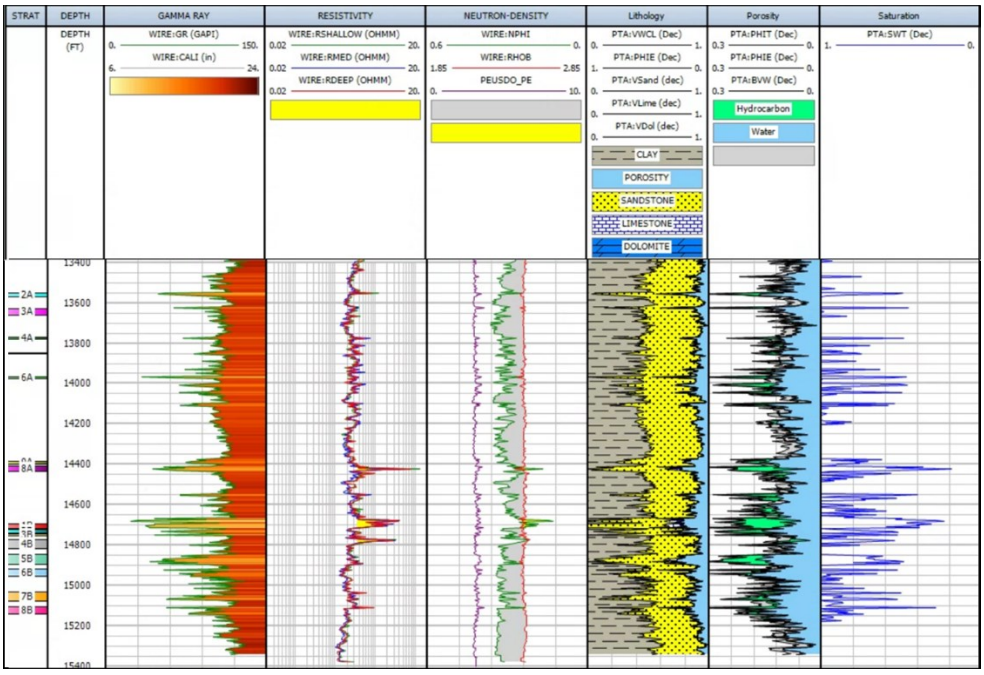

Figure 10: Last track on right demonstrates the total water saturation interpretation where 1 =100% water-filled and 0 = hydrocarbon-filled.

The uncertainty in interpreted total water saturation is +/-15% (0.15). To identify the most water-prone zones for the geothermal production potential in net reservoir a cutoff of ~75% or > was applied. By doing so a net 'pay' criteria is established to guide prospecting efforts and ensure that water-prone/dominated production will result from any exploratory or development efforts.

3.2 Temperature and Pressure Gradients

Loucks et al. (1981) analyzed information from wells in the Deep Frio sandstones in Texas Gulf Coast. In this study, there was found two pressure gradient zones; the normal ("soft") geopressure zone, with a pressure gradient of 10.52 kPa/m (0.465 psi/ft), and a "hard" hydropressured zone that start from 2440 m to 3,650 m of 15.83kPa/m (0.7 psi/ft). As the target zone is placed in the Deep Frio Sandstones, the reservoir is located in the high-pressure zone, with a reservoir pressure of 54 MPa.

Texas Gulf Coast is located in a zone identified with hydrothermal potential (Fig. 11, right). Temperature gradient varies with depth (Fig. 11, left). Loucks et al. (1981), determined two temperature gradients in the Deep Frio sandstones in Texas Gulf Coast; in the soft geopressured zone the geothermal gradient is 24.6°C/km (1.35°F/100 ft), and in the hard hydropressured zone the geothermal gradient rises to 45.4°C/km (2.49°F/100 ft). This effect is attributed to the abnormal rock compaction that increases the effective thermal conductivity in that region.

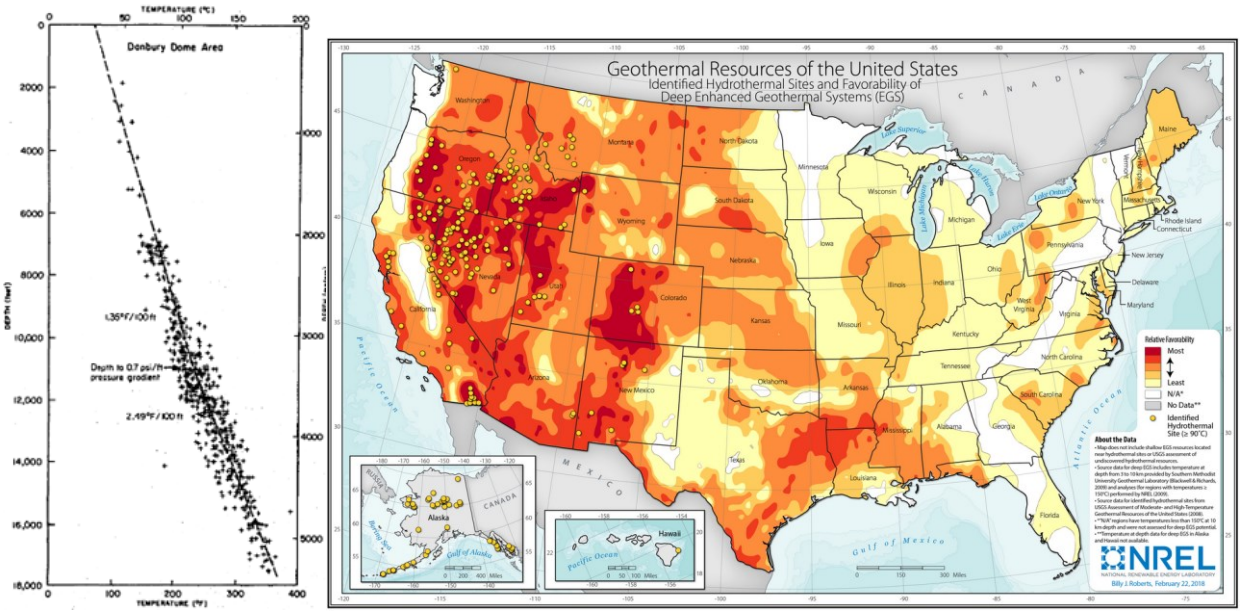

Figure 11: Temperature versus depth, Texas Gulf Coast (Loucks et al. 1981) [left]. Map of the geothermal resources in the United States (Roberts, 2018) [right].

4. RESERVOR MODEL

The reservoir was built in a grid that covers an area of 10,670 m by 10,670 m equivalent to 113.8 sq-km (1.225 E6 sq-ft). The depth of the grid varies from 3950 m to 4680 m, with a total thickness of 730 m. To better represent the petrophysical properties, we used a relatively fine grid that covered the area previously described with a total of 242176 cells (44(i) x 43(j) x 128(k)). Sequential gaussian simulation was used as the modeling method. The permeability and porosity models, we focused on the 4 subintervals of the Frio Formation that were selected based on their optimal properties (porosity, permeability, and water saturation), although the connecting zones between intervals of interest were modeled as well to assess the heat flow vertically among targets. Fig. 12 shows a representative well with a display of the original permeability and porosity logs with their correspondent upscaled to the grid log using the arithmetic averaging method. The Fig. 13 and Fig. 14 show porosity and permeability of the region modeled. Petrophysical properties visualization provides valuable resource to evaluate potential wells placement. Applying appropriate petrophysical cut-offs highlights reservoirs of interest with optimal petrophysical properties and high water saturations that deliver suitable water production.

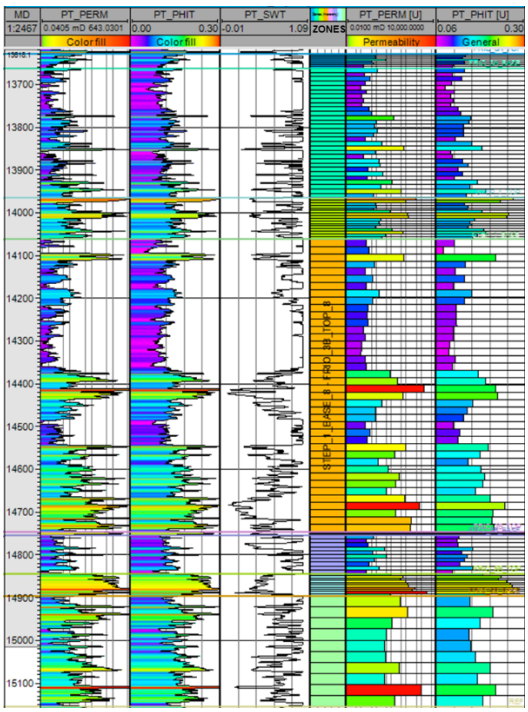

Figure 12: Petrophysical properties.

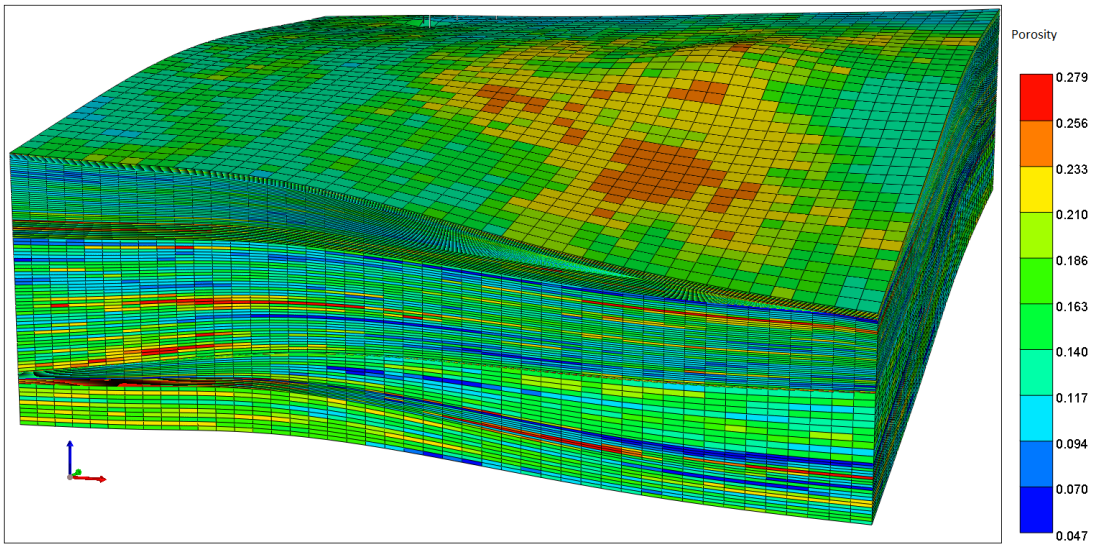

Figure 13: Porosity of the grid.

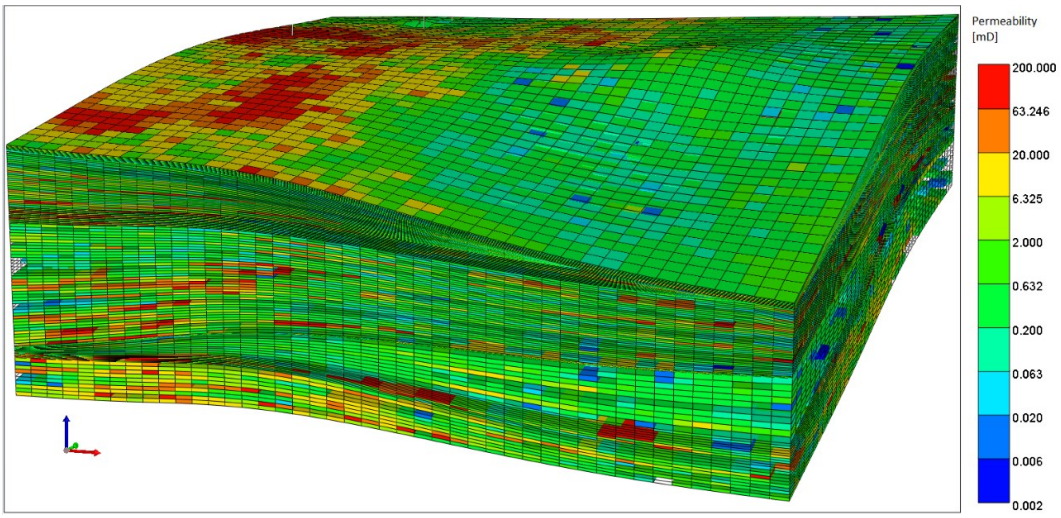

Figure 14: Permeability of the grid.

The geothermal gradient of the model was generated with the geothermal gradient of the Texas Gulf Coast wells based on Loucks et al. (1981) study (Fig. 15). In this case the average reservoir temperature of the region of interest is around 150°C.

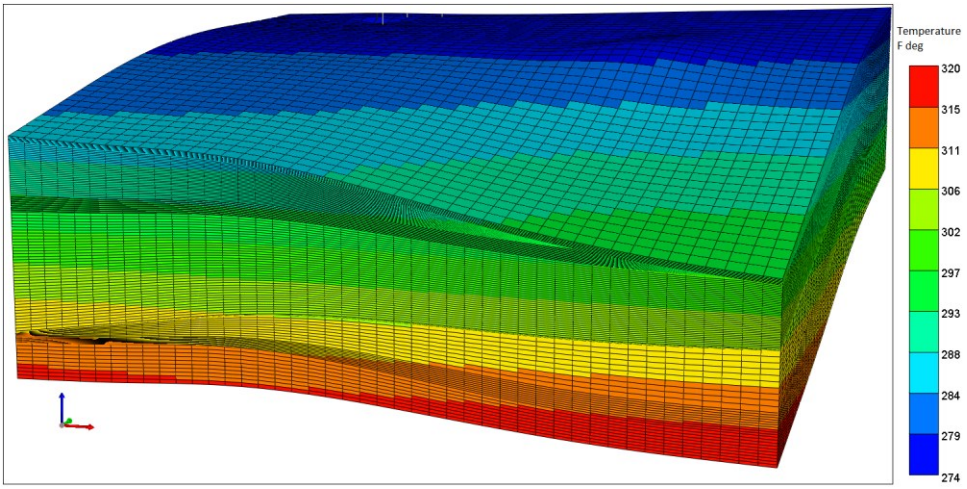

Figure 15: Temperature of the grid in °F.

5. ENTHALPY PRODUCTION FORECAST AND FIELD POTENTIAL

Simulations were performed to 30 years of water production. Simulation parameters are depicted in Table 1. In these simulations the injection rate is equivalent to the production rate. The intention is to preserve the reservoir pressure.

Table 16: Simulation Parameters.

Parameter	Value/Description
Simulation time	30 Years
Injection Wells	4 vertical existing wells
Production wells	1 new horizontal well (1220m horizontal displacement)
Injection rate	27.5 liters/s per well
Production rate	110 liters/sec
Water Reinjection Temperature	40°C

To understand the impact of the production well placement, 2 different production well locations were evaluated (Fig. 16). In the configuration 1, the production well is located 1 km east from the injection area. In the configuration 2, the production well was placed 2 km in the south direction from the injection area. As mentioned earlier, the placement of the injector wells are fixed since they are existing wells.

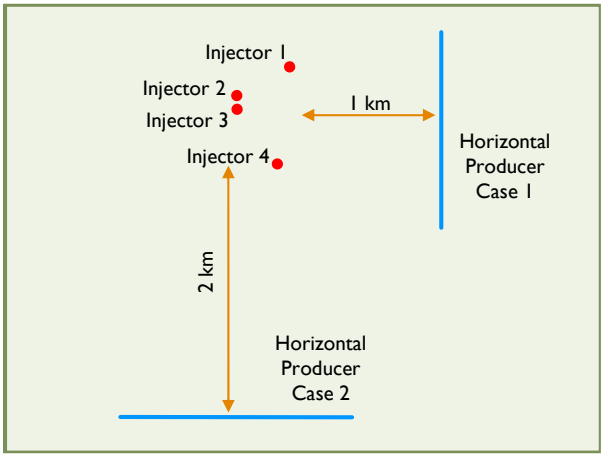

Figure 17: Well configurations evaluated.

The results of the simulation show that well placement has an impact in the enthalpy production (Fig 17). As observed in the figure, after 30 years of production in the case 1, the cold front from the water injected in the existing wells reaches the drainage area of the horizontal well. In Fig. 19, it is possible to see the impact in enthalpy production. The energy production was calculated based on a geothermal power plant utilization efficiency of 12%. This efficiency is in the low range of subcritical Organic Rankine cycle, making this model conservative. As seen in the Fig 19, the energy production in the configuration 1 starts to decline at the 10th year of production, showing the impact of the cold front. As a result, with the time the reservoir temperature in the drainage region of the producing well is declining, reducing the enthalpy production.

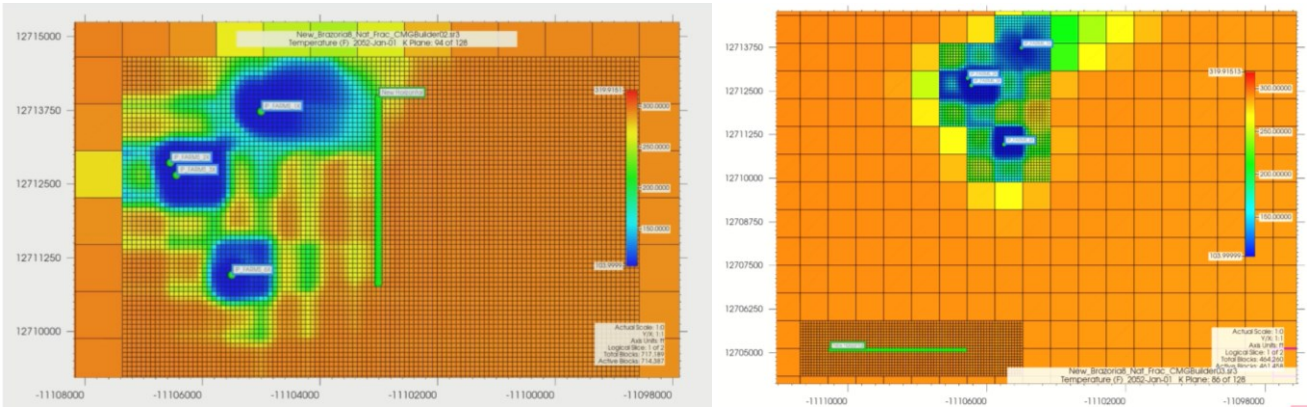

Figure 18: Cold temperature front evolution in the configuration 1 (left), and the configuration 2 (right) after 30 years of production.

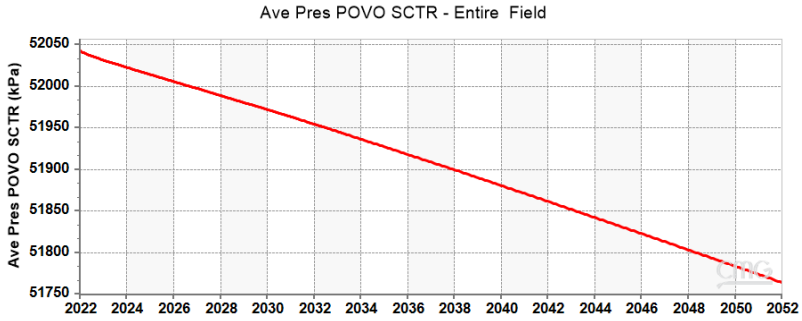

Figure 19: Reservoir pressure declination.

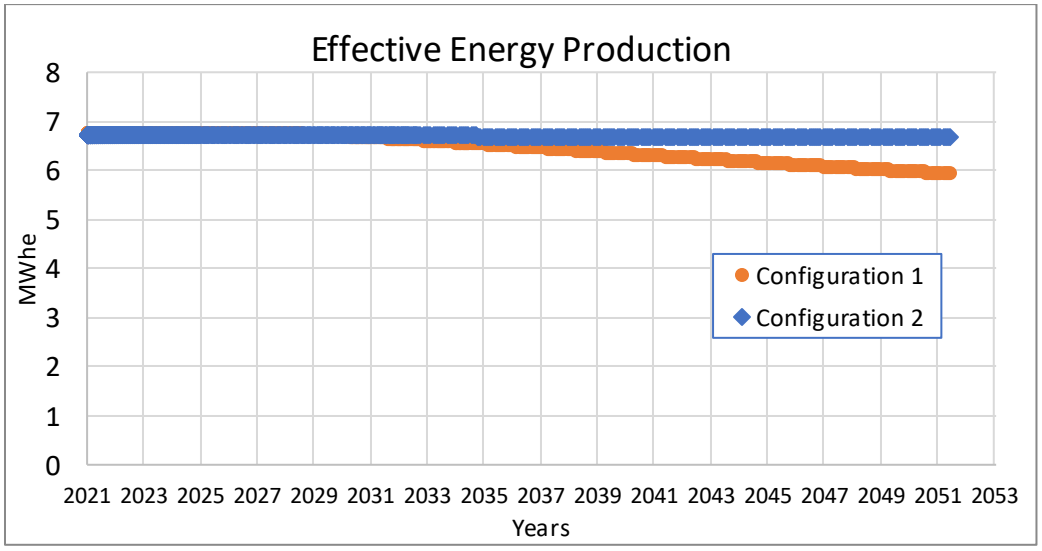

Figure 20: Effective energy production for the 2 configurations analyzed.

As seen in the production plots, in the configuration 2 the reservoir is capable to produce around 6.7MWh during 30 years.

6. GEOPHIRES/ECONOMICAL MODEL

Reservoir simulation thermal energy outputs were applied directly in the Geophires v2.0 geothermal technoeconomic simulation tool (Beckers et al. 2018) to estimate levelized cost of energy (LCOE) including both electricity and thermal energy use cases. The thermal energy applied from the reservoir source to the final net conversion of electricity depends on several factors including flow rate, well and surface friction, well thermal properties, wellhead to heat sink distance, fluid types, parasitic plant and reinjection load, and thermal

efficiency of turbomachinery. These factors are not explored in depth during this study although assumptions are taken here to estimated net production of power and heat generated energy sold.

The facility end use option considered included combined heat and power topping cycle with electricity as the main product and heat sales thereafter. An electricity only model was also evaluated. Outputs are highly dependent on assumptions for parasitic load and other factors impacting system and plant efficiency. Total capital cost ranging from $15 million to $20 million were assumed leading estimated outputs for LCOE between 3.0 cents/kWh and 9.6 cents/kWh.

7. CONCLUSION

This study proposes a novel method of using abandoned oil or gas wells for injection and a new horizontal well for heat extraction in a hot sedimentary basin. Water was used as the working fluid. The wells analyzed are in Texas Gulf Coast, where at the target depth, temperatures of 150°C enable power production. Power of 6 MW could be generated using a wellbore depth of 4100 m with a flow rate of 110 l/s.

The distance between injector and producer can affect the energy output. In this case, numerical simulation provides good support of the distance required to avoid the cold front from injector wells reaching the drainage area of the producer well.

Abandoned oil and gas wells in hot sedimentary basins can facilitate access to geothermal energy, supporting the high capital costs that constrain the expansion of this renewable energy source. Economic projects are achievable using similar development methodology and present an attractive opportunity to realize a renewable energy source in a way that hasn't been achieve previously.

REFERENCES

Anderson, T. (2013). Geothermal potential of deep sedimentary basins in the United States. In Unconventional Resources Technology Conference, pages 1969–1978. Geothermal Resources Council Transaction.

Archie, G. E. 1952. Classification of carbonate reservoir rocks and petrophysical considerations: AAPG Bulletin, vol. 36, no. 2, p. 218–298

Bebout, D.G., Loucks, R.G. and Gregory, A.R., 1978. Frio sandstone reservoirs in the deep subsurface along the Texas Gulf Coast-their potential for production of geopressured geothermal energy. University of Texas Bureau of Economic Geology.

Beckers KF, McCabe K. Introducing GEOPHIRES v2.0: Updated geothermal techno-economic simulation tool. In: Proceedings, 43rd workshop on geothermal reservoir engineering, Stanford University, Stanford, California, February 12-14, 2018, SGP-TR 213. 2018.

Bethke, S. Altaner, W. Harrison, C. Upson. 1988. Supercomputer analysis of sedimentary basins. Science, 239 (4837) (1988), pp. 261-267. https://www.jstor.org/stable/pdf/1700720.pdf

Bu, X., Ma, W. and Li, H., 2012. Geothermal energy production utilizing abandoned oil and gas wells. Renewable energy, 41, pp.80-85.

Caulk, R.A. and Tomac, I., 2017. Reuse of abandoned oil and gas wells for geothermal energy production. Renewable energy, 112, pp.388-397.

Cheng, W.L., Li, T.T., Nian, Y.L. and Wang, C.L., 2013. Studies on geothermal power generation using abandoned oil wells. Energy, 59, pp.248-254.

Davis, A.P., and Michaelides, E.E. 2009. Geothermal power production from abandoned oil wells. Energy, 34 (2009), pp. 866-872. https://doi.org/10.1016/j.energy.2009.03.017.

Fisher, W. L., 1969, Facies characterization of Gulf Coast Basin delta systems, with Holocene analogues: Gulf Coast Assoc. Geol. Socs. Trans., v. 19, p. 239-261.

Gharibi, S., Mortezazadeh, E., Bodi, S.J.H.A. and Vatani, A., 2018. Feasibility study of geothermal heat extraction from abandoned oil wells using a U-tube heat exchanger. Energy, 153, pp.554-567.

Kujawa, T., Nowak, W. and Stachel, A.A., 2004. Utilization of existing deep geological wells for acquisitions of geothermal energy. In Thermal Sciences 2004. Proceedings of the ASME-ZSIS International Thermal Science Seminar II. Begel House Inc.

Loucks, R.G., Richmnn, D. L., and Milliken K. L. 1981. Factors Controlling Reservoir Quality in Tertiary Sandstones and Their Significance to Geopressured Geothermal Production (No. DOE/ET/27111-T3). Texas Univ., Austin (US). Bureau of Economic Geology (US).

Morton, R.A., 1979. Characteristics of Shallow Subsurface Faults on Texas Inner Shelf. AAPG Bulletin, 63(3), pp.498-499.

Roberts, B.J., 2018. Geothermal Resources of the United States. National Renewable Energy Laboratory (NREL) map. https://www.nrel.gov/gis/assets/images/geothermal-identified-hydrothermal-and-egs.jpg.

Vivas, C., Salehi, S., Tuttle, J., and Rickard, B. 2020. Challenges and Opportunities of Geothermal Drilling for Renewable Energy Generation. GRC Transactions, Vol. 44, (2020), 904-918.